Coherent Control of Harmonic Generation in Superlattices: Single-Mode Response

Kirill A. Pronin[1,2] and Andre D. Bandrauk[2]

[1]*Institute of Biochemical Physics, Russian Academy of Sciences, Moscow 119 991, Russia*
[2]*Faculte des Sciences, Universite de Sherbrooke, Sherbrooke J1K 2R1, Quebec, Canada*

(Received 14 November 2005; published 13 July 2006)

We study the harmonic generation spectrum in a semiconductor superlattice (a quantum-dot array) at slow relaxation. The effect of a single-mode response in an alternating rectangular (meander) electric field is demonstrated: For certain values of field parameters, the extremely wide discrete output spectrum with slowly decaying tails (multiharmonic generation) shrinks to one single harmonic (single-harmonic generation). Similarly, the effect is manifested in the transient continuous spectrum by diminishing the divergencies (peaks) at all odd harmonics but one. Substantial control over the spectrum is demonstrated.

DOI: 10.1103/PhysRevLett.97.020602 PACS numbers: 05.60.Gg, 68.65.Cd, 73.21.Cd, 78.67.Pt

Coherent control of atoms, molecules, and solids [1,2], a new promising area of research, addresses manipulation of the electronic properties (electric current, localization, harmonic generation, etc.) by tuning the parameters of the applied field. In atomic or molecular systems, high-order harmonics are generated due to ionization and recollision processes in a strong laser field, accompanied by formation of a plateau in the spectrum [3]. Another plateau emerges within the two-level model of ''doorway'' states [4]. In solids, coherent control of electric currents and harmonic spectra has been demonstrated both in theory and in experiment [5–14]. The phase between the components of the applied ''colored'' field can be used to manipulate both the magnitude and the polarity of the current produced [7–9,11,13,14]. Induced localization can also be controlled through the parameters of the applied field [5,6,14]. The formation of plateaus in high-harmonic spectra of solids has been demonstrated [6,10,12,13], with the cutoff determined by the field magnitude. Sparse harmonic generation spectra have been found in ring molecules or crystals interacting with a circularly polarized laser field [15] and in atoms interacting with two-color circularly polarized laser fields [16]. Of special interest for coherent control are semiconductor superlattices and quantum-dot arrays [17] (along with optical lattices [18]), which make possible the observation of coherence effects in crystalline-type systems with the use of accessible dc fields and terahertz ac fields.

In this Letter, we study the harmonic generation spectra in semiconductor superlattices. We show that the spectrum of response in a rectangular alternating field has the shape of a peak with very slowly decaying tails [6], in contrast to conventional plateaus in smooth fields [3,4,6,10,12,13]. The primary result of the Letter is to demonstrate that, by tuning the parameters of the applied wide-spectrum input field, a controllable transition from a wide-spectrum response (multiharmonic generation) to a single-mode response (single-harmonic generation) is possible.

Let us consider a d-dimensional conductor (a semiconductor [17] or optical [18] superlattice, a quantum-dot array [17]) with a cubic-type lattice within a one-band approximation. We adopt the tight-binding approach with possible overlap $H^{(0)}_{\mathbf{0},\mathbf{n}}$ between sites $\mathbf{n}$. The system is exposed to an alternating rectangular space-homogeneous electric field (a meander, series of square pulses with time period T, basic frequency $\omega = 2\pi/T$):

$$\begin{aligned} \mathbf{E}(t) &= \mathbf{E}, \qquad -T/4 < t - mT < T/4, \\ \mathbf{E}(t) &= -\mathbf{E}, \qquad T/4 < t - mT < 3T/4, \end{aligned} \tag{1}$$

where m is any integer. The field (1) is not weak with respect to the bandwidth, so the treatment is nonlinear and nonperturbative in its amplitude $\mathbf{E}$.

The problem is solved analytically in the general form for any time $t = mT + \Delta t$ within the stochastic Liouville equation or the kinetic Boltzmann relaxation-time approach [14]. This is an adequate framework for semiconductor superlattices [17] in the nearly coherent regime of slow relaxation $\alpha T \ll 1$, where α is the relaxation rate. The electron thermalizes with the characteristic time scale α^{-1}; the probability of scattering during the period of the field T is low. The nonlinear ac response to the field (1) in the leading order in αT for the entire time range follows from Eq. (8) of Ref. [14] (periodic case in the absence of dc field):

$$\mathbf{j}(mT + \Delta t) = -e[e^{-\alpha m T}\hat{\mathbf{D}}_0 + (1 - e^{-\alpha m T})\hat{\mathbf{K}}_0]v(\Delta t), \tag{2}$$

$$\begin{aligned} v(-T/4 \le \Delta t \le T/4) &= \sin(\mathbf{n}\boldsymbol{\varepsilon}\omega\Delta t), \\ v(T/4 \le \Delta t \le 3T/4) &= -\sin[\mathbf{n}\boldsymbol{\varepsilon}(\omega\Delta t - \pi)], \end{aligned} \tag{3}$$

where $\mathbf{j}$ is the electric current, e is the modulus of the electron charge, $\boldsymbol{\varepsilon} = e\mathbf{E}a/\hbar\omega$, and a is the intersite distance. The operator coefficients $\hat{\mathbf{D}}_0$ and $\hat{\mathbf{K}}_0$ sum up the oscillations over wave vectors $\mathbf{k}$ and over sites $\mathbf{n} = n^i\mathbf{a}_i$:

$$\hat{\mathbf{D}}_0 = \frac{2}{\hbar}\sum \mathbf{n} H^{(0)}_{\mathbf{0},\mathbf{n}} \int d\mathbf{k}\, \frac{\rho_{\mathbf{k},\mathbf{k}}(0)}{V_{\mathrm{BZ}}} \cos(\mathbf{k}\mathbf{n}), \tag{4}$$

$$\hat{\mathbf{K}}_0 = \frac{4N_e}{\pi\hbar}\sum \frac{\mathbf{n}}{\mathbf{n}\boldsymbol{\varepsilon}} \sin\left(\mathbf{n}\boldsymbol{\varepsilon}\frac{\pi}{2}\right) H^{(0)}_{\mathbf{0},\mathbf{n}} \int d\mathbf{k} f(\mathbf{k}) \cos(\mathbf{k}\mathbf{n}). \tag{5}$$

Here V_{BZ} is the volume of the Brillouin zone, N_e is the

electron density, and $f(\mathbf{k})$ is the equilibrium distribution function. The initial density matrix we assume symmetric, $\rho_{\mathbf{k},\mathbf{k}}(0) = \rho_{-\mathbf{k},-\mathbf{k}}(0)$. The term with $\hat{\mathbf{D}}_0$ provides the transient dynamic regime, while $\hat{\mathbf{K}}_0$ corresponds to the emerging kinetic regime [14].

For simplicity, we project the motion on the x direction (evolution along different axes is uncorrelated) and adopt the nearest-neighbor approximation $|n| = 1$.

The harmonic spectrum of the nonstationary current (2)–(5) consists of (a) a discrete component $\mathbf{j}_d$, coming from the stationary periodic long-time kinetic evolution and (b) a continuous transient component $\mathbf{j}_c$ from the relaxation process.

The discrete spectrum $\mathbf{j}_d$ incorporates only odd harmonics and in the main term is α-independent:

$$\mathbf{j}_d(mT + \Delta t) = -e\hat{\mathbf{K}}_0 v_d(\Delta t), \tag{6}$$

$$v_d(\Delta t) = \frac{4}{\pi}\varepsilon\cos\left(\frac{\pi\varepsilon}{2}\right)\sum_{\nu=1}^{\infty}\frac{(-1)^{\nu+1}}{(2\nu-1)^2-\varepsilon^2}\sin[(2\nu-1)\omega\Delta t]. \tag{7}$$

The typical shape of it reveals a peak at order close to ε with long spectral tails—the harmonic amplitudes decay slowly with increasing order $\sim\nu^{-2}$ (Fig. 1). The extended width of the spectrum of response agrees well with the intuitive picture: The input field (1) has a wide spectrum $\sim\nu^{-1}$. The output spectrum is expected to be wide as well. The nonlinear frequency-mixing processes contribute to the widening of it.

However, there exists a special regime, when this wide output spectrum collapses into one single mode (Fig. 1). This drastic change happens when ε takes any integer odd value:

$$\varepsilon = 2\tilde{\nu} - 1 = \text{odd}, \tag{8}$$

where $\tilde{\nu}$ is some integer. Then the discrete spectrum (6) instead of (7) retains only one single harmonic:

$$v_{\mathrm{SMR}}(\Delta t) = \sin[(2\tilde{\nu} - 1)\omega\Delta t], \tag{9}$$

all the others being exactly zero within the considered leading term $\sim(\alpha T)^0$. In other words, the tuning of the amplitude or frequency of the input field (1) enables a controllable transition from a wide-spectrum response (7) to a single-mode response (SMR) [Eq. (9)]. Somewhat counterintuitively, the response to a multiharmonic input field consists then of a single spectral line. This transition in the spectrum takes place by all the harmonic amplitudes sinking, except for the single one of order $2\tilde{\nu} - 1$, the amplitude of which remains constant (Fig. 1).

The origin of the effect can be observed from the time evolution (2) and (3). At the discontinuities of the input field (1), $t_\Delta = [(1/4) + (m'/2)]T$, the (continuous) ac response (3) typically acquires a cusp—discontinuity of the acceleration, $\partial j(t_\Delta - 0)/\partial t = -\partial j(t_\Delta + 0)/\partial t$. It is this cusp (Fig. 2) that gives rise to the wide spectrum (7)—in contrast to plateaus in smooth fields [3,4,6].

The values (8) for SMR are special in the fact that the oscillations (3) in the two half-periods not only match but coincide entirely (Fig. 2). The cusp disappears, and the oscillations form one single harmonic (9)—one single line in the discrete spectrum. In fact, under Eq. (8) the electron velocity for the state k before the discontinuity t_Δ coincides exactly with the velocity in the state $-k$ after the discontinuity. The contributing states and velocities before and after t_Δ become exactly similar, provided the initial band filling $\rho_{k,k}(0)$ was symmetric in k. Relaxation does not destroy the effect as the typical interscattering time exceeds the period of the field.

More insight can be obtained by noting that the frequency of this single harmonic $\varepsilon\omega$ is nothing but the frequency of Bloch oscillations $\omega_0 = eEa/\hbar$ in the constant fields $\pm E$ at the upper and lower steps of the meander. Under condition (8), the half-period of the input field $T/2$ (the step of the meander) comprises a half-integer number of Bloch periods, which makes possible their exact matching. Furthermore, the accelerations at the time of the field discontinuities t_Δ vanish exactly under Eq. (8), becoming

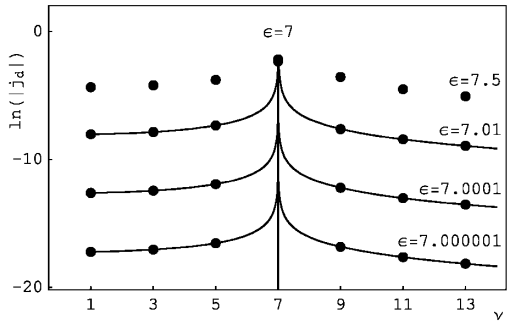

FIG. 1. Discrete ac spectra j_d (log plot, arbitrary units) vs harmonic order ν: transition from a wide-spectrum ($\varepsilon = 7.5$, upper dots) [Eqs. (6) and (7)] through $\varepsilon = 7.01$, 7.0001, 7.000001 to a single-mode response ($\varepsilon = 7$, single dot, same magnitude) [Eq. (9)]. Continuous curves serve as guidelines only.

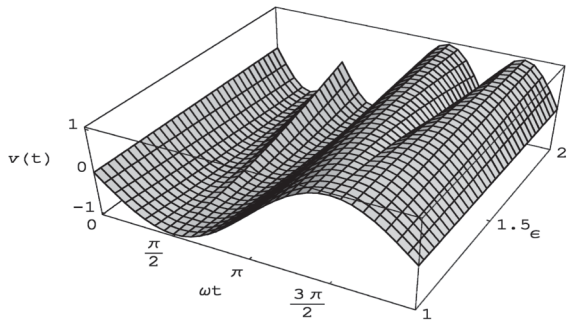

FIG. 2. Current oscillation $v(t)$ [Eq. (3)] (arbitrary units) as a function of ωt within a period T, a function of ε. Transition from cuspless oscillation at $\varepsilon = 1$ (SMR, $\varepsilon = $ odd) through intermediate values with cusps, $1 < \varepsilon \leq 2$, to vanishing kinetic spectrum at $\varepsilon = 2$ (induced localization, $\varepsilon = $ even).

insensitive to the abrupt inversion of the sign of the field (1). All these ingredients form a single smooth oscillation without cusps [Eq. (9) and Fig. 2].

Coherent control of the harmonic spectrum through the SMR effect is obviously different from the traditional manipulation through the transparency band of the media. For example, here the frequency of the single generated harmonic is not fixed by the properties of the media but can be controlled by the amplitude of the field. The nature of these two effects is also different—in the present case, it originates from nonlinearity and coherence.

Another effect takes place if the field parameters satisfy

$$\varepsilon = 2\tilde{\nu} = \text{even}. \tag{10}$$

Then, due to the vanishing of the kinetic factor $\hat{\mathbf{K}}_0$ [Eq. (5)], the leading terms $\sim(\alpha T)^0$ of the discrete spectrum (6) vanish entirely. Tuning of the amplitude or frequency (1) in the vicinity of the values (10) enables coherent control of the discrete (or long-time kinetic) harmonic generation spectrum up to its total collapse. This collapse happens by uniform vanishing of all harmonic amplitudes. It originates from the averaging of the electron velocity in the kinetic regime over the field period for the account of scattering and provides another manifestation of field-induced localization [5,14]. The cusps at t_Δ under Eq. (10) remain (Fig. 2).

The continuous transient spectrum $\mathbf{j}_c$ comprises the decay of the dynamic and the onset of the kinetic regime in the entire time range:

$$\mathbf{j}_c(t) = -e(\hat{\mathbf{D}}_0 - \hat{\mathbf{K}}_0)\int_0^\infty d\Omega v_c(\Omega)\sin(\Omega\omega t), \tag{11}$$

$$v_c(\Omega) = \frac{2\alpha\varepsilon\cot(\pi\Omega)[\cos(\pi\Omega/2) - \cos(\pi\varepsilon/2)]}{\omega\cos(\pi\Omega/2)(\Omega^2 - \varepsilon^2)}. \tag{12}$$

Here the frequency Ω is measured in units ω and, thus, corresponds to harmonic order.

The amplitude $v_c(\Omega)$ is small in α in contrast to the discrete spectrum v_d (7). However, $v_c(\Omega)$ is the leading term in between the integer harmonics (Fig. 3). For ε noninteger, the continuous spectrum (11) exhibits divergencies of two types: (i) linear divergencies (antiresonances) $v_c(\Omega) \sim \xi^{-1}$ in the vicinity of even harmonics, $\Omega = 2\nu + \xi$, $\xi \ll 1$, and (ii) quadratic divergencies (resonances) $v_c(\Omega) \sim \xi^{-2}$ in the vicinity of odd harmonics, $\Omega = 2\nu - 1 + \xi$. At $\Omega = \varepsilon$ there is no divergence. For antiresonances $\sim\xi^{-1}$, the harmonic amplitudes change sign at $\Omega = 2\nu$, so that their contributions compensate each other in part. In contrast to that, the resonances $\sim\xi^{-2}$ are stronger and enhance the harmonics $\Omega = 2\nu - 1$. That correlates qualitatively with the fact that the discrete spectrum $\mathbf{j}_d$ consists of odd harmonics solely.

The SMR effect (8) changes the continuous spectrum (11) profoundly. We find then (i) linear divergencies $v_c(\Omega) \sim \xi^{-1}$ in the vicinity of all integer harmonics, both even and odd, $\Omega = \nu + \xi$, and (ii) quadratic divergence $v_c(\Omega) \sim \xi^{-2}$ in the vicinity of the only SMR harmonic (8), $\Omega = 2\tilde{\nu} - 1 + \xi$. The SMR effect decreases the odd harmonics down to the order of even ones, except for the single mode $\Omega = 2\tilde{\nu} - 1$. This change is one order in magnitude—this time one order in the deviation ξ instead of one order in the small relaxation rate α, as it was in the discrete spectrum. All integer harmonics become weak antiresonances, except for the single mode $2\tilde{\nu} - 1$, which remains a strong resonance and interferes positively. Thus, the SMR effect is also well pronounced in the continuous spectrum [Fig. 3 (dotted curves)].

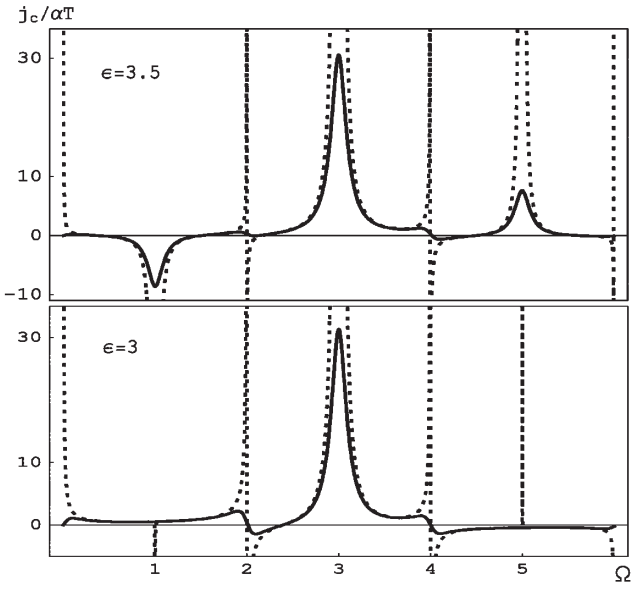

FIG. 3. Continuous harmonic spectra j_c (arbitrary units), scaled by αT, vs harmonic order Ω: transition from resonances at $\Omega =$ odd and smaller antiresonances at $\Omega =$ even for $\varepsilon = 3.5$ (upper plot, $\varepsilon \neq$ odd) to all small antiresonances with the only nonsmall SMR resonance for $\varepsilon = 3$ (lower plot, SMR, $\varepsilon =$ odd). The dotted curves are for $\alpha \to 0$, solid curves $\alpha = 0.1$.

The induced localization (10), despite the profound effect upon the discrete spectrum (5)–(7), influences the continuous spectrum (11) and (12) less—due to the inherent presence of the dynamic contribution $\hat{\mathbf{D}}_0$. Apart from the entire vanishing of the kinetic term (5) in Eq. (11), it modifies the selected harmonic $2\tilde{\nu}$: (i) The divergence at $2\tilde{\nu}$ disappears. (ii) The divergencies at even harmonics, other than $2\tilde{\nu}$, remain linear. (iii) The divergencies at all odd harmonics remain quadratic.

The appearance of divergencies in the continuous spectrum is due to the slow-relaxation limit. Beyond it, the resonant denominators get renormalized:

$$(\Omega - \varepsilon)^2 \to (\Omega - \varepsilon)^2 + (\alpha/\omega)^2, \tag{13}$$

$$\sin(\pi\Omega)\cos(\pi\Omega/2) \to \frac{\sin^2(\pi\Omega) + (\pi\alpha/\omega)^2}{2\sin(\pi\Omega/2)}. \tag{14}$$

The divergencies get smoothed [Fig. 3 (solid curves)] into big resonances and small antiresonances. The SMR effect

is highly pronounced through the height of these peaks: In the general case (non-SMR), the amplitudes of the odd-order resonances are large as $\sim\alpha^{-1}$ as compared to small $\sim\alpha$ off-resonance values. They decay with the increase of the SMR order $(2\tilde{\nu}-1)$ and of the deviation $|\nu-\tilde{\nu}|$, retaining the α^{-1} dependence for all. Under SMR (8), the height of the only main resonance is similarly large in the relaxation rate, and it also decreases with SMR order $\nu_{\mathrm{SMR}}\sim(\alpha/\omega)^{-1}(-1)^{\tilde{\nu}}(2\tilde{\nu}-1)^{-1}$. However, this time the SMR effect washes out all the other resonances $\nu\neq\tilde{\nu}$ by 2 orders—down to $\sim\alpha$. The amplitudes of the antiresonances (at all even orders) in all the cases are $\sim\alpha^0$, i.e., an order smaller than that of resonances—in correlation with the odd-harmonics nature of the discrete spectrum. The SMR effect in the smoothed spectrum is revealed clearly.

Additional insight can be obtained from the time profile of the spectrum, measured or calculated over the field period T or at least over an interval shorter than the relaxation time α^{-1} (which may be much longer than T) at some time $t=mT+\Delta t$. In the leading order, the electron evolution (2) is quasistationary (periodic) within $\omega\Delta t\ll(\alpha T)^{-1}$. Consequently, the time profile of the spectrum is discrete and it is provided by Eqs. (2) and (7). We note readily the time invariance of its shape—it is independent of m apart from the overall factor in Eq. (2). The reciprocal magnitudes of different harmonics, measured both in the dynamic (short-time) and in the kinetic (long-time) regimes, as well as in the transition process, are alike. This is a notable fact, as in other aspects these regimes are very different (cf. Ref. [14]).

The spectrum time profile supports entirely the SMR effect—under the condition (8) its wide discrete spectrum (7) collapses into one single harmonic (9) as above. This similarity originates from the quasistationary time invariance of the evolution within the time scale α^{-1} compared to the exact long-time periodicity. Under SMR, the collapse takes place throughout the entire time range, any m in Eq. (2), or, upon scanning the field parameters, at the moment Eq. (8) is satisfied.

The existence of the SMR effect both in the discrete spectrum (6) and (7) and in the time profile of the spectrum (2) and (7) is understandable, as the transition from cusp-like evolution to cuspless oscillation takes place within each period irrespective of the time interval for averaging. The continuous spectrum (11) and (12), however, is of the next order in the small parameter α, so the SMR effect upon it was not guaranteed.

Under induced localization (10), the only surviving dynamic contribution $\hat{\mathbf{D}}_0$ (4) to the spectrum profile decays with the time scale $\sim\alpha^{-1}$, so that at long time $\alpha t\gg 1$ in the main term all harmonic amplitudes vanish.

Discontinuous time-dependent fields as in Eq. (1) are idealizations of fast-changing fields with smoothed steps. Smoothing of the discontinuities within a narrow time interval δt, $\delta t/T\ll 1$ does not destroy the effect but adds to the SMR harmonic a tail, small with $\delta t/T$.

To summarize, we have demonstrated the effect of a single-mode response in an alternating rectangular (meander) electric field. This wide-spectrum input field enables, upon tuning of its parameters, a controllable transition from multiharmonic generation to single-harmonic generation. The suitable systems are semiconductor superlattices or quantum-dot arrays. The mechanism is provided by the nonlinear intraband evolution in the nearly coherent regime. As discussed in Ref. [14], the requirements for the observation of the effect are feasible. In a separate publication, based on Ref. [14], we demonstrate that there exists a range of parameters where domain splitting does not occur, which could otherwise preclude the observation of SMR effect in the steady state (cf. Ref. [19]). The SMR effect provides a clear example and a tool for substantial coherent control over the ac response or harmonic generation spectrum. We believe it will be of interest for the construction of sensors of electromagnetic radiation in the terahertz range, for the generation, conversion, and measurement of frequencies and for digital information processing in optoelectronics.

The authors gratefully acknowledge financial support from NSERC (Canada).

[1] *Coherent Control in Atoms, Molecules, and Semiconductors*, edited by W. Poetz and A. Schroeder (Kluwer, Dordrecht, 1999).
[2] M. Shapiro and P. Brumer, *Principles of the Quantum Control of Molecular Processes* (Wiley, New York, 2003).
[3] P. B. Corkum, Phys. Rev. Lett. **71**, 1994 (1993).
[4] T. Zuo, S. Chelkowski, and A. D. Bandrauk, Phys. Rev. A **48**, 3837 (1993); **49**, 3943 (1994).
[5] D. H. Dunlap and V. M. Kenkre, Phys. Rev. B **37**, 6622 (1988).
[6] K. A. Pronin, A. D. Bandrauk, and A. A. Ovchinnikov, Phys. Rev. B **50**, R3473 (1994); J. Phys. Condens. Matter **6**, 4721 (1994); Synth. Met. **71**, 1687 (1995).
[7] E. Dupont *et al.*, Phys. Rev. Lett. **74**, 3596 (1995).
[8] R. Atanasov *et al.*, Phys. Rev. Lett. **76**, 1703 (1996).
[9] A. Hache *et al.*, Phys. Rev. Lett. **78**, 306 (1997).
[10] M. W. Feise and D. S. Citrin, Appl. Phys. Lett. **75**, 3536 (1999).
[11] K. A. Pronin and A. D. Bandrauk, Phys. Rev. B **69**, 195308 (2004).
[12] V. I. Litvinov and A. Manasson, Phys. Rev. B **70**, 195323 (2004).
[13] T. M. Fortier *et al.*, Phys. Rev. Lett. **92**, 147403 (2004).
[14] K. A. Pronin, P. Reineker, and A. D. Bandrauk, Phys. Rev. B **71**, 195311 (2005).
[15] O. E. Alon, V. Averbukh, and N. Moiseyev, Phys. Rev. Lett. **80**, 3743 (1998).
[16] F. Ceccherini, D. Bauer, and F. Cornolti, Phys. Rev. A **68**, 053402 (2003).
[17] A. Wacker, Phys. Rep. **357**, 1 (2002).
[18] G. Grynberg and C. Robilliard, Phys. Rep. **355**, 335 (2001).
[19] H. Kroemer, cond-mat/0009311.